

Design of a Quasi-Passive Knee Exoskeleton to Assist Running

Aaron M. Dollar, *Member, IEEE*, and Hugh Herr, *Member, IEEE*

Abstract— In this paper we describe the design and preliminary evaluation of an energetically-autonomous powered knee exoskeleton to facilitate running. The device consists of a knee brace in which a motorized mechanism actively places and removes a spring in parallel with the knee joint. This mechanism is controlled such that the spring is in parallel with the knee joint from approximately heel-strike to toe-off, and is removed from this state during the swing phase of running. In this way, the spring is intended to store energy at heel-strike which is then released when the heel leaves the ground, reducing the effort required by the quadriceps to exert this energy, thereby reducing the metabolic cost of running.

I. INTRODUCTION

WORK in the area of lower-limb exoskeletons began primarily in the late 1960s, almost in parallel between a number of research groups in the United States and in the former Yugoslavia. These efforts were split between developing technologies to augment the abilities of able-bodied humans, often for military purposes [1,2], and developing assistive technologies for handicapped persons [3,4]. Despite the differences in intended use, these two fields face many of the same challenges and constraints, particularly related to portability and interfacing closely to a human operator.

Within the last decade, research in the area of exoskeletons and active orthoses has experienced a revival. A number of the more significant efforts in the field include exoskeletons such as BLEEX [5], Sarcos' exoskeleton [6], and HAL [7], as well as active orthotic devices such as those by Herr [8], Ferris [9], Sugar [10], and Agrawal [11]. See [12] for a thorough review of research in the area of exoskeletons for both assistive technology (active orthoses) and for augmenting the abilities of able-bodied wearers such as soldiers.

A small number of exoskeleton and orthotic devices have been developed for specific application to the knee (e.g. [13,14]). The work most similar to our knee exoskeleton concept is the Roboknee (Yobotics, Inc., Cincinnati, OH, USA), a simple exoskeleton for adding power at the knee to assist in stair climbing and squatting during load-carrying tasks [15]. The device consists of a linear series-elastic actuator connected to the upper and lower portions of a knee

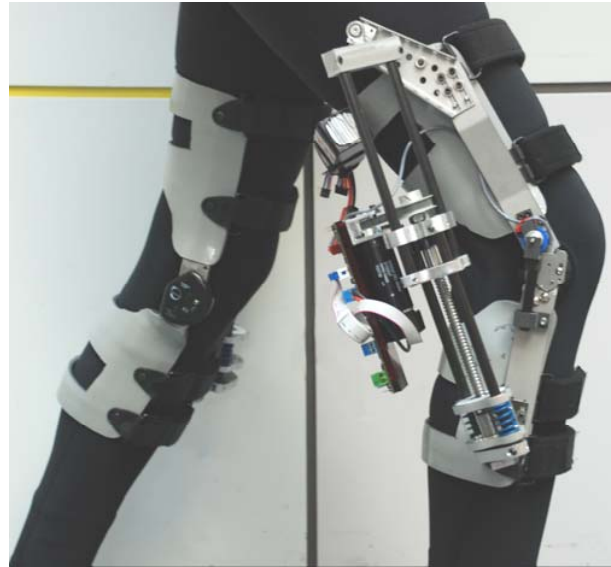


Fig. 1. Exoskeleton prototypes being worn by a user.

brace, just below the hip and on the calf, respectively. The control of the RoboKnee utilizes the ground reaction force (in the vertical direction) and the center of pressure in the sagittal plane (front/back direction) to create a positive-feedback force amplification control scheme of the torque at the knee.

In contrast to the RoboKnee, we describe a quasi-passive device that does not add mechanical power at the knee, but rather stores and releases energy in a spring that is actively placed/removed from being in parallel with the biological joint. This approach provides a natural low impedance to the user and allows for a simple position-control scheme of the actuator. Furthermore, our device is intended to aid the wearer in running, reducing metabolic cost of transport and fatigue of the wearer. As far as we are aware, no active exoskeleton or orthotic device to date has been specifically designed to assist running.

In the following sections, we begin with a description of some of our previous work that partially motivates the current concept, followed by a brief background on the biomechanics of human running. We then present our design concept, describing the working principle, detailed design information, and preliminary benchtop evaluation of the hardware prototypes. Finally, we present a discussion of the concept, identifying the challenges and potential pitfalls of successful exoskeletons and how these apply to our design.

A. M. Dollar is with the Harvard/MIT Division of Health Sciences and Technology and the MIT Media Lab, Massachusetts Institute of Technology, Cambridge, MA 02139 USA (e-mail: adollar@mit.edu).

H. Herr is with the MIT Media Lab and the Harvard/MIT Division of Health Sciences and Technology, Massachusetts Institute of Technology, Cambridge, MA 02139 USA (corresponding author phone: 617-314-3661; fax: 617-253-8542; e-mail: hherr@media.mit.edu).

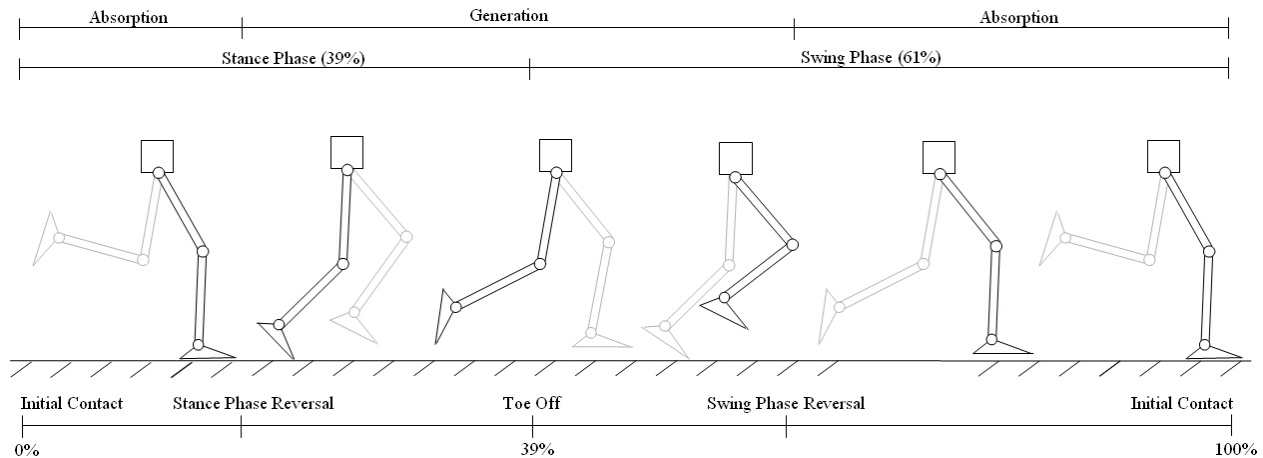


Fig. 2. Human running gait through one cycle, beginning and ending at heel strike (initial contact). Percentages showing contact events are given at their approximate location in the cycle. Adapted from [18].

II. MOTIVATION AND PREVIOUS WORK

In previous work in our lab we developed a quasi-passive exoskeleton device intended to exploit the passive dynamics of human walking in order to create lighter and more efficient exoskeleton devices. The exoskeleton does not actively add power at the joints of the wearer. Instead, the design relies on the controlled release of energy stored in springs during the negative power phases of the walking gait [16]. The quasi-passive elements in the exoskeleton (springs and variable damper) were chosen based on an analysis of clinical gait analysis (CGA) data.

Without a payload, the exoskeleton weighed 11.7kg and required only 2 Watts of electrical power during loaded walking. For a 36 kg payload, we demonstrated that the quasi-passive exoskeleton transferred on average 80% of the load to the ground during the single-support phase of walking. By measuring the rate of oxygen consumption on a study participant walking at a self-selected speed, we found that the exoskeleton slightly increased the walking metabolic cost of transport (COT) as compared to a standard loaded backpack (10% increase). However, a similar exoskeleton without joint springs or damping control (zero-impedance exoskeleton) is found to increase COT by 23% compared to the loaded backpack, highlighting the benefits of passive and quasi-passive joint mechanisms in the design of efficient, low-mass leg exoskeletons.

While these were not the desired results, it is thought to be the first reported study on the metabolic cost associated with walking under the aid of an exoskeleton. Additionally, these results were confirmed in a recent study conducted at the U.S. Army Natick Soldier Center with another quasi-passive exoskeleton. This study showed that load-carriage using the Natick exoskeleton device increased metabolic COT across all three tested loading conditions (20 kg, 40 kg,

and 55 kg) by as much as 60% [17].

As will be discussed, humans are much less efficient at running than walking. We believe that this inefficiency allows for opportunities to improve human running more easily than walking, since a relatively small amount of metabolic power saved by the device will have a large effect on the energy required to perform the task. Furthermore, by saving this energy, the operator will remain aerobic in muscle metabolism for a longer amount of time, allowing him/her to run longer and/or faster without fatigue.

III. BIOMECHANICS OF RUNNING

Before getting into the details of the design of our exoskeleton device, it is important to provide a brief background on the biomechanics of human running, as this information plays a crucial role in the design of such systems. Fig. 2 (adapted from [18]) shows a simplified diagram of human running gait, with terms that will be used throughout this paper. Note that the timing of the labeled events during the gait cycle is approximate, and varies across individuals and conditions. The human running gait cycle is typically represented as starting (0%) and ending (100%) at the point of heel strike (initial contact) on the same foot, with heel strike on the adjacent foot occurring at approximately 50% of gait cycle.

Note that since the stance phase per leg is less than 50% of the gait cycle (39% in this example, but can vary with subject and conditions), there exists two aerial periods of the gait cycle in which neither foot is touching the ground – directly after ‘toe off’ and directly before ‘initial contact’. Each of these periods last approximately 11% of the gait cycle. Typically, the change between walking and running is considered to be the point at which the gait cycle changes from having periods of double support (both feet on the ground) to periods of double float (neither foot on the

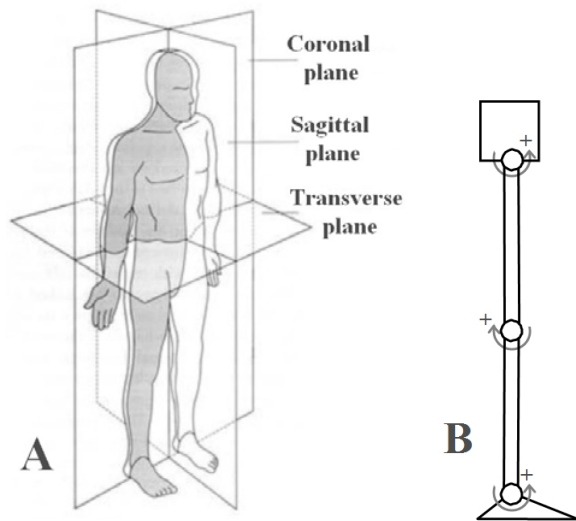


Fig. 3. Description of the anatomical planes (A) and a diagram of the leg shown in the rest position (0 deg at all joints) with the positive direction indicated (B).

ground). Furthermore, the distinction between running and sprinting is such that, in the former, initial contact is made with the hindfoot (heel), versus forefoot contact in the latter.

Also indicated on Fig. 2 are the approximate points when the body is transitioning between phases of acceleration (generation) and deceleration (absorption), referred to as “stance phase reversal” and “swing phase reversal”. Note that these transitions happen in between contact events, with the leg first absorbing energy and then generating energy between initial contact and toe off. This generated energy accelerates the body during swing directly after toe off until swing phase reversal, at which point deceleration begins.

Fig. 3 shows a description of the human anatomical planes (Fig. 3A) as well as a kinematic model of the human leg in the sagittal plane, which is the dominant plane of motion during human locomotion (Fig. 3B). Note the convention of the knee angle, shown at zero degrees with the positive direction indicated.

Fig. 4 shows the typical behavior of the knee during normal, level-ground running at 3.2 m/s (scaled for an 85kg subject), adapted from [18]. Note that the plots related to knee angle and torque were adapted directly from [18], whereas the velocity was obtained by differentiating the adapted angle data, and the power by multiplying the adapted torque and velocity data (inverted to make absorptive power appear as negative power).

Fig. 5 shows the energy cost per unit distance as a function of speed for walking and running (adapted from [19]). During walking, the preferred speed of humans unsurprisingly falls within the minimum at around 1.1-1.4 m/s as shown in the figure, with energy cost varying little within this range. As speed increases past this range, the cost of walking increases, until eventually it becomes more efficient to run. However, running at any speed requires

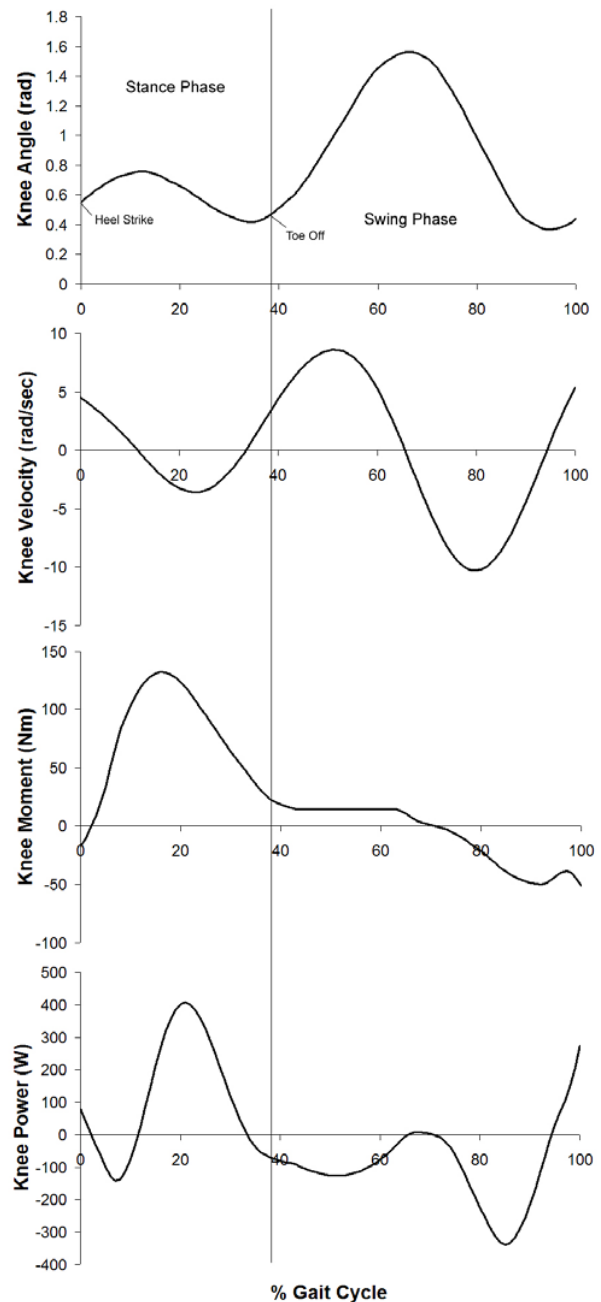


Fig. 4. Biomechanics of the knee of an 85kg individual running at 3.2 m/s showing knee joint angle, velocity, moment, and power (adapted from [18]).

approximately 25% more energy per unit distance than walking at the preferred speed.

IV. WORKING PRINCIPLE

The concept of storing and releasing energy in elastic mechanisms to aid in ambulation is not new. Most commercial prosthetic feet consist of carbon fiber leaf springs that store energy at heel strike that is released during late stance. A large number of the exoskeleton concepts

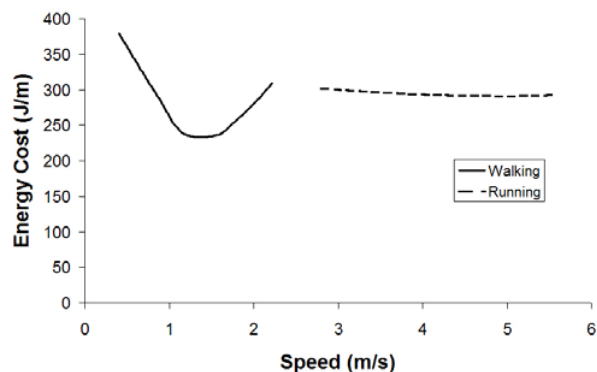


Fig. 5. Energy cost per unit distance as a function of speed for walking and running (adapted from [21]).

described in [12] utilize passive springs in the ankles and/or hips. A concept presented in [20] describes an “exoskeleton” consisting of artificial elastic tendons spanning multiple joints, meant to harness negative (dissipative) energy at one joint and transfer it to another as positive energy. However, in all of these concepts the springs are always in the system, without movable set points. For the knee, however, this approach is impractical, as the joint goes through the angles in which an elastic element is desired twice (once during stance, the desired phase, and once during swing, when the spring should not resist the joint motion – see Fig. 4 top).

The running knee exoskeleton is intended to be used in the following way: at approximately 3% of the gait cycle (knee angle of 36deg for the given gait data), the spring should begin to be compressed and continue as the knee flexes. During this period of the ‘absorption’ phase of the running gait, the spring compresses and provides the negative power that the muscles acting on the knee (primarily the quadriceps) would otherwise need to provide, until the point of maximum flexion during stance is reached (at approximately 14% of the gait cycle at a knee angle of 44deg for the given gait data). At this point the knee begins to extend again, with the torque on the knee due to the spring decreasing and adding the energy stored as positive power to the joint until the knee has extended back through the 36deg spring set point, at approximately 22% of the gait.

The torque and power on the biological joint due to the spring compression is shown in Fig. 6 as the shaded areas. Note that the peak spring torque is less than the peak biological torque since this point occurs after peak knee flexion during stance has occurred, or approximately 16% of the gait cycle. Also note that the spring stores nearly the entire amount of the negative power during the absorptive stance phase, which is then immediately released as positive power during the generative stance phase.

Integrating the data from Fig. 4 bottom, the knee provides about 47.9J of positive (generative) mechanical power and 59.7J of negative (absorptive) mechanical power during one

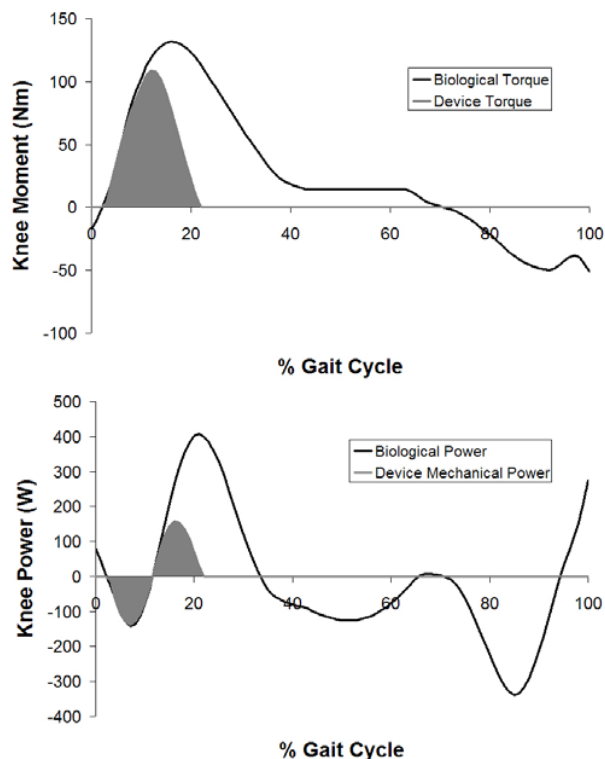


Fig. 6. Mechanical properties of the exoskeleton design as a function of running gait percentage.

gait cycle. Assuming that all other aspects of the running ambulation remain the same (and they would almost certainly not remain the same in practice), the current design could potentially save the knee 7.8J of positive mechanical energy and 6.1J of negative mechanical energy, or 19% and 11% respectively. Given the fact that running is approximately 25% more energetically expensive per unit distance than walking, these numbers are significant. Furthermore, positive muscle power is approximately four times more metabolically expensive than negative power, making the result even more significant [21].

In practice we will likely not see the full improvement shown above due to a number of practical considerations, many of which are discussed in section VI. However, there is great potential for a device that reduces the effort required for running, regardless of the degree of that reduction.

V. DEVICE DESIGN

Fig. 7 shows a representative diagram of the running knee exoskeleton concept. A pair of raceways that slide with respect to one another are connected to a thigh and calf brace mount. A passive slide with a contact plate is attached to the thigh of the device, and a motor-positioned spring is attached to the shank. This spring carriage is servoed to avoid contact with the upper slide during the swing phase of the gait, and to come into contact with the slide and cause

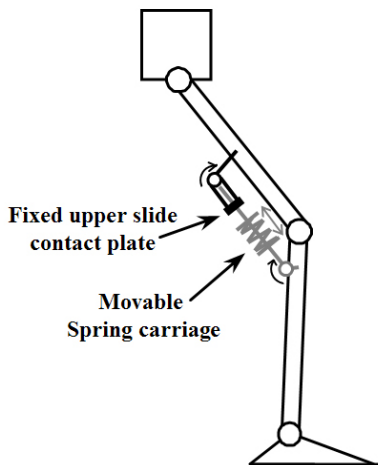


Fig. 7. Representative diagram of the running knee exoskeleton concept.

compression of the springs during the appropriate parts of the stance phase.

A solid model of the full spring/actuator module is shown in Fig. 8. A brushed DC motor actuates the nut via a belt drive and ball screw. The motor and mounting hardware are placed as high in the module as possible to minimize inertial loading of the leg by the device. Note that the carriage containing the die springs is attached directly to the ball screw nut in this design (as opposed to the layout in Fig. 7) and is servoed up and down with the movement of the upper slide to contact the bottom surface of the 'upper slide'.

The motor is stalled to support the force of the compressed spring. In the first iteration of this prototype a 60W DC motor (RE 30, Maxon Motor, Switzerland) is used for this purpose. The actuator module shown in Fig. 8 attaches to the thigh 25cm above the knee and 16cm below the knee. For these values a die spring stiffness of approximately 110 kN/m is required to produce the peak torque needed. These values result in the torque and power profiles shown in Fig. 5.

The rails of the actuator modules are made from carbon fiber tubing to minimize weight. Rulon bearings are used to create a low friction sliding surface. The entire actuator module, including motor and all transmission components weighs approximately 1.0 kg.

In order to achieve good alignment with the knee of the operator and a comfortable interface, custom-fitted knee braces configured for this application were fabricated. These braces have physical stops to keep the range of motion safely within 0-100 degrees of flexion. Unlike typical knee braces, the hard cuffs are to the rear of the user's legs in order to support and distribute the spring forces that tend to extend the knee. These cuffs are a hybrid composite material to minimize weight, and the joints are a heavy-duty joint designed for rugged post-polio braces in order to support the loads and bending moments exerted by

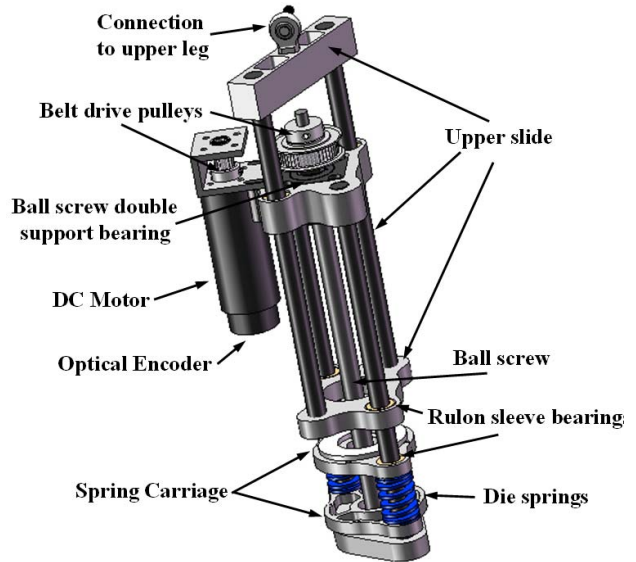


Fig. 8. CAD model of the actuator module.

TABLE I
DESIGN SPECIFICATIONS

Gear ratio (motor/spring carriage)	1mm/rot
Allowable range of knee joint motion	0-97 deg
Total gear ratio (motor/knee) @ 0 deg	112
Total gear ratio (motor/knee) @ 97 deg	947
Individual Spring stiffness	54.6 kN/m
Total Spring stiffness	109.3 kN/m
Max Continuous Force @ 24V	524 N
Max continuous torque at 44 deg	47.5 Nm
Intermittent (Stall) Force	6.4 kN
Operating Voltage	24 V

the actuator modules, which are mounted to the outside of each leg. The braces are made using joint hardware and a kit from Townsend Design (Bakersfield, CA, USA). Due to the actuator module being located to the side of the leg and the easy Velcro straps, the exoskeleton device can be donned in approximately 30 seconds, and doffed in about 5 seconds.

The braces currently weigh 1.18 kg each, the majority of which is due to the heavy-duty joint and added actuator support brackets. The exoskeleton prototypes, consisting of the actuators, braces, and control hardware, can be seen in Figs. 1, 9, and 10.

A. Design Specifications

Table I shows the design specifications of the actuator module, assembled with the knee brace. A 3:1 belt drive steps the motor speed down before the ballscrew, which has a lead of 3mm, resulting in a total step-down ratio from the motor of 1mm linear carriage travel per rotation of the motor. In its current mounting configuration, the exoskeleton has a 97 degree range of motion from full knee extension (per Fig. 3B), allowing for the full 90 degree

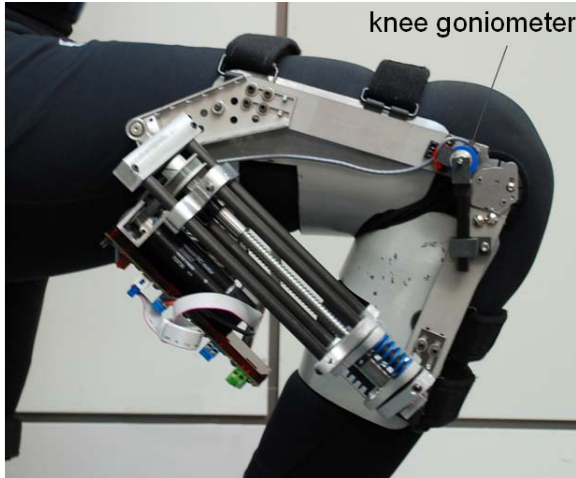


Fig. 9. Image of one of the exoskeleton prototypes (right leg) showing the range of motion and the shortest actuator length.

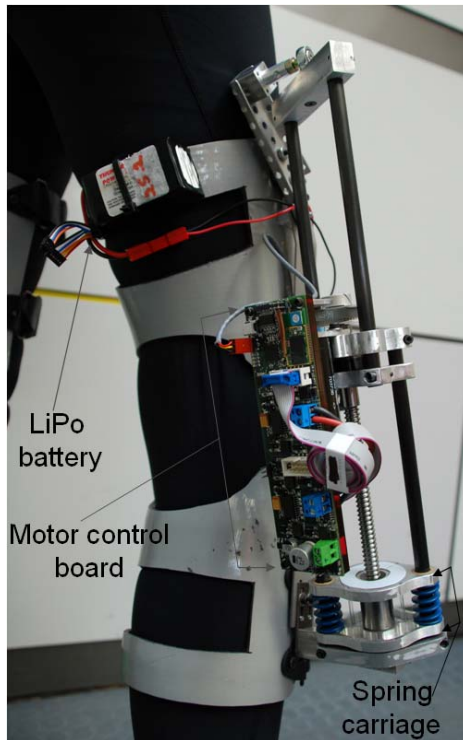


Fig. 10. Battery and control hardware.

range of knee flexion during running according to the data in Fig. 4. Due to the actuator alignment, the total transmission ratio from motor to knee joint varies from 112 to 947 across this 97 degree range of motion.

As per the specifications of the motor (RE 30, 24V, 60W, Maxon Motor, Switzerland) and the actuator transmission ratio, the maximum continuous linear actuator force is approximately 524N, which corresponds to 47.5 Nm at 44deg knee flexion (when maximum actuator load is predicted). Since the average torque required by the device over one gait cycle is 12.0 Nm (Fig. 6), the chosen design

TABLE II
PHYSICAL PARAMETER SPECIFICATIONS

Actuator length range	0.27m-0.40m
Actuator Stroke	0.13 m
Connection location above knee	0.25 m
Connection location below knee	0.16 m
Angular offset of above knee location	10 deg
Contact surface area thigh	290 sq.cm
Contact surface area calf	283 sq.cm
Additional width (from external brace joint)	0.103 m
Lever arm from knee joint	0.070 m
Mass Parameters	
Carriage mass	694 g
Motor, control board mass	408 g
Battery mass	185 g
Brace mass	1179 g
Total Exoskeleton mass	2466 g

parameters put the motor well within its safe operating range.

Table II gives the relevant physical parameters of the exoskeleton prototype. Note the large contact area of the brace on the user over which the actuator load is distributed, ensuring a more comfortable fit. The total exoskeleton mass is just under 2.5 kg per leg, approximately half of which is due to the brace. This value includes the power source (battery), control electronics, and actuator for the energetically autonomous and portable device.

B. Control

The exoskeleton will be controlled by estimating the gait phase and knee angle using the optical encoder on the motor shaft and a rotary potentiometer on the joint of the brace. Ground contact events will be detected using a footswitch-based insole in the operator's shoes (B&L Engineering, Tustin, CA, USA). For the purposes of this application, only the sensor located in the heel of the insole will be used to indicate heel strike.

These sensors will be used to implement position control of the spring carriage. The two primary control states are fixing the position of the carriage during the spring compression phase (i.e. stalling the motor) and tracking of the upper slide contact plate during the swing phase of gait. Currently, the actuator is not used to add mechanical power to the user, but is quasi-passive.

The control of the exoskeleton will be implemented using custom built DSP microcontroller-based hardware (Fig. 10). The electronics are completely stand-alone and portable, consisting of a single board with three analog input channels, and two motor control channels, including an encoder counter. The motor controller currently operates in voltage control mode, with a 100 KHz PWM and voltage loop bandwidth only limited by that of the actuator.

The control electronics exist as a small, stand-alone

TABLE III
PERFORMANCE MEASURES

Frictional torque at knee @ 44 deg	~0.25 Nm
Load required to backdrive the carriage (3:1 belt)	~180 N
Max Spring carriage speed (@24V, 3:1 belt)	128 mm/sec
Rise time to max velocity (@24V, 3:1 belt)	0.15 sec
Max Spring carriage speed (@24V, 2:1 belt)	187 mm/sec
Max Spring carriage speed (@30V, 2:1 belt)	240 mm/sec

package, approximately 41mm x 151mm x 10mm (1.6" x 6.0" x 0.4"), and weighs approximately 20g. This hardware requires a low quiescent power of approximately 2W. To keep weight low, high power-density Lithium Polymer batteries are being used (Thunder Power, Las Vegas, NV, USA), providing approximately 150 W-hours/kg of power (top left corner of Fig. 10).

VI. EVALUATION

Table III shows the results of a number of bench tests of the prototype actuator. The torque on the knee due to friction during free swinging of the joint was found to be on the order of 0.25Nm – approximately 1/600 of the maximum moment on the joint during running (Fig. 4). The load required to backdrive the actuator was found to be approximately 180N, which serves to reduce the torque required by the motor to fix the spring carriage during stance.

The application of the device to the task of running presents an interesting challenge in that both the maximum continuous torque and “no-load” speed limits of the actuator are both being approached at different phases of the gait (friction and inertia still presents a sizable load to the actuator during high velocities and accelerations). During stance, the load on the spring carriage must be supported by stalling the motor. Furthermore, the spring carriage must be quickly moved away during the swing phase in order to allow the knee to freely flex. The choice of the transmission ratio therefore becomes a crucial factor in balancing these rigorous performance requirements.

According to the data in Fig. 4 and the chosen design parameters, the spring carriage must be moved 102mm in 0.286sec to allow the knee to freely swing after the energy stored in the springs during early stance has been returned to the wearer during late stance. This motion occurs between 22% and 66% of the gait cycle, and requires an average spring carriage velocity of 357 mm/sec.

Figure 11 shows the step response of the actuator module to a positional step command of 40mm at time zero for a belt drive step-down ratio from the motor of 3:1 (for a total actuator transmission ratio of 1mm per motor rotation) and a 24V supply. These results show a maximum velocity of 128 mm/sec with a ramp-up time of 0.15 seconds – an average of 95 mm/sec for 0.286 sec. This maximum speed was increased to 187 mm/sec by changing the belt ratio to 2:1, and was further increased to 240 mm/sec by increasing the

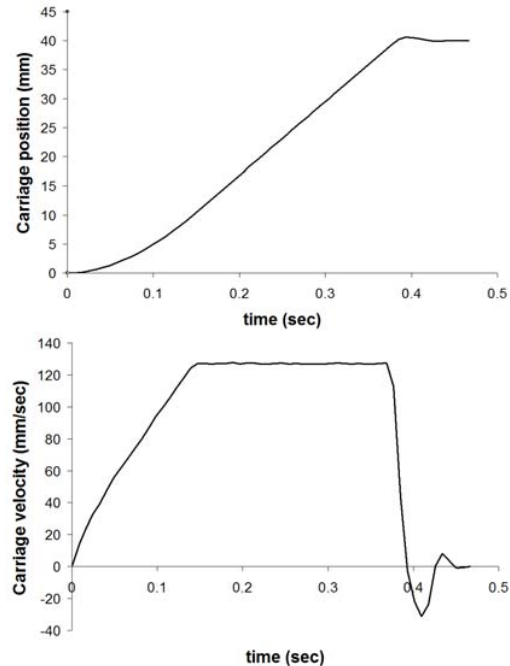


Fig. 11. Spring carriage position and velocity for a step displacement of 40mm. Test was run at 24V with a 1mm per motor revolution transmission ratio.

supply voltage to 30V. By pushing the supply voltage to 36V, we expect 283 mm/sec accordingly. Furthermore, we decreased the ramp up time from 0.15sec to 0.04sec by using LiPo batteries, which can source current much faster than the external power supply used in the tests shown in Fig. 11. Fig. 12 shows the current required during a similar step response test, with an average of 1.25 amps during steady state motion at 128 mm/sec.

We are currently implementing the hardware to further lower the step-down ratio, and expect to be able to achieve the desired average velocity to allow the carriage to servoed to allow the knee to swing without being impeded. However, since this actuator is being pushed towards its limit, we are also building control hardware to utilize the Maxon EC-Powermax 30 (Maxon Motor, Switzerland), a 200W brushless DC motor of similar size but with more than twice the nominal speed. This particular motor presents a control challenge due to its low inductance that we are currently addressing.

VII. DISCUSSION

In addition to those mentioned above, there are a great number of other challenges associated with demonstrating an effective exoskeleton device. A number of design issues may lead to poor performance: misalignment of joints between operator and hardware, kinematic constraints from attachments such as harnesses and cuffs, design not optimized for running gait, added forces to the operator that resist motion, and addition of power in a sub-optimal

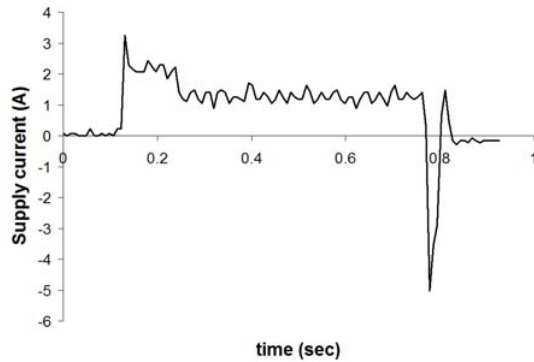


Fig. 12. Supply current for a carriage step displacement of 40mm. Test was run at 24V with a 1mm per motor revolution transmission ratio.

manner (e.g. mistiming, too little, too much), among others.

For our specific application, two major considerations are immediately apparent. First, the mass of the exoskeleton should be kept as low as possible, and should be concentrated close to the hip of the user, in order to minimize the added inertia on the legs and therefore the metabolic effort associated with moving that mass. Second, one of the greatest challenges related to our concept is the small flexion angle of the knee through which the spring is compressed (approximately 8deg for the given gait data). This fact highlights the importance of good calibration of the device for the specific user, an accurate control scheme that allows the nut to closely track the end of the spring, as well as a transmission with little backlash.

One key performance measure in demonstrating the effectiveness of our performance-augmenting exoskeleton is metabolic cost of transport (COT). By measuring the oxygen consumption and carbon dioxide production of human breathing during a task, a measure of how physically taxing the activity is to the subject can be gotten [22,23]. We will use the K4 telemetric system (Cosmed srl, Rome, Italy) [24] to compare the metabolic COT between running with and without the exoskeleton device, as well as with an equivalent added mass and inertia to the legs in order to determine whether there is any energetic advantage to using the device. We are currently awaiting approval to begin human-subjects studies to evaluate the effectiveness of the device.

ACKNOWLEDGMENTS

The authors would like to thank Lee Magnusson for his assistance on the knee design and solid modeling, Karina Pikhart for her assistance during the fabrication of the devices, Grant Elliot for his assistance with the control electronics, and to Lifestyle Prosthetics for their assistance with the fitting and construction of the knee braces.

REFERENCES

[1] R.S. Mosher, "Handyman to Hardiman," SAE Technical Report 670088, 1967.

[2] J.A. Moore, "Pitman: A Powered Exoskeleton Suit for the Infantryman," Los Alamos National Laboratory Technical Report LA-10761-MS, 1986.

[3] M. Vukobratovic, B. Borovac, D. Surla, and D. Stokic, *Scientific Fundamentals of Robotics 7, Biped Locomotion: Dynamics Stability, Control, and Application*. New York: Springer-Verlag, 1990.

[4] A. Seireg and J.G. Grundmann, "Design of a Multitask Exoskeletal Walking Device for Paraplegics," *Biomechanics of Medical Devices*, Marcel Dekker, Inc, New York, pp. 569-644, 1981.

[5] A.B. Zoss, H. Kazerooni, and A. Chu, "Biomechanical Design of the Berkeley Lower Extremity Exoskeleton (BLEEX)," *IEEE/ASME Transactions on Mechatronics*, vol. 11(2), pp. 128-138, 2006.

[6] E. Guizzo and H. Goldstein, "The Rise of the Body Bots," *IEEE Spectrum*, October, 2005.

[7] H. Kawamoto, Suwoong Lee, S. Kanbe, and Y. Sankai, "Power assist method for HAL-3 using EMG-based feedback controller," *proceedings of the IEEE International Conference on Systems, Man, and Cybernetics*, pp. 1648-1653, 2003.

[8] J. Blaya and H. Herr, "Adaptive Control of a Variable-Impedance Ankle-Foot Orthosis to Assist Drop-Foot Gait," *IEEE Transactions on Neural Systems and Rehabilitation Engineering*, vol. 12(1), pp. 24-31, 2004.

[9] G.S. Sawicki, K.E. Gordon, D.P. Ferris, "Powered Lower Limb Orthoses: Applications in Motor Adaptation and Rehabilitation," *Proceedings of the 2005 IEEE International Conference on Rehabilitation Robotics (ICORR)*, pp. 206-211, 2005.

[10] K. Bharadwaj, T.G. Sugar, J.B. Koeneman, E.J. Koeneman, "Design of a Robotic Gait Trainer using Spring Over Muscle Actuators for Ankle Stroke Rehabilitation," *Transactions of the ASME, Journal of Biomechanical Engineering*, vol. 127, pp. 1009-1013, 2005.

[11] A. Agrawal, S.K. Banala, S.K. Agrawal, S.A. Binder-Macleod, "Design of a Two Degree-of-freedom Ankle-Foot Orthosis for Robotic Rehabilitation," *Proceedings of the 2005 IEEE International Conference on Rehabilitation Robotics (ICORR)*, pp. 41-44, 2005.

[12] A.M. Dollar and H. Herr, "Lower-Extremity Exoskeletons and Active Orthoses: Challenges and State of the Art", *IEEE Transactions on Robotics*, vol. 24(1), pp. 144-158, 2008.

[13] C. Mavroidis et al., "Smart Portable Rehabilitation Devices," *Journal of Neuroengineering and Rehabilitation*, vol. 2(18), 2005.

[14] G.T. Huang, "Wearable Devices Add Strength," *Technology Review*, pp. 26, Feb. 2004.

[15] J.E. Pratt, B.T. Krupp, C.J. Morse, and S.H. Collins, "The RoboKnee: An Exoskeleton for Enhancing Strength and Endurance During Walking," *Proc. IEEE International Conference on Robotics and Automation*, New Orleans, LA, USA, pp. 2430-2435, 2004.

[16] C.J. Walsh, K. Endo, H. Herr, "Quasi-passive leg exoskeleton for load-carrying augmentation," *International Journal of Humanoid Robotics*, 2007 (in press).

[17] K.N. Gregorczyk et al., "The Effects of a Lower Body Exoskeleton Load Carriage Assistive Device on Oxygen Consumption and Kinematics during Walking with Loads," *25th Army Science Conference*, Orlando, FL, USA, Nov. 27-30, 2006.

[18] T. Novacheck, "The Biomechanics of Running," *Gait and Posture*, vol. 7, pp. 77-95, 1998.

[19] R.M. Alexander, "Running. The Human Machine." Natural History Museum Publications, London, pp. 74-87, 1992.

[20] A.J. van den Bogert, "Exotendons for Assistance of Human Locomotion," *BioMedical Engineering Online*, vol. 2, 2003.

[21] R. Margaria, "Biomechanics and Energetics of Muscular Exercise," Clarendon Press, Oxford, UK, 1976.

[22] J.M. Brockway, "Derivation of formulae used to calculate energy expenditure in man," *Human Nutrition: Clinical Nutrition*, vol. 41, pp. 463-471, 1987.

[23] J.M. Donelan, R. Kram, and A.D. Kuo, "Mechanical work for step-to-step transitions is a major determinant of the metabolic cost of human walking," *Journal of Experimental Biology*, vol. 205, pp. 3717-3727, 2002.

[24] C. Hausswirth, A.X. Bigard, and J.M. Lechevelier, "The Cosmed K4 telemetry system as an accurate device for oxygen uptake measurement during exercise," *International Journal of Sports Medicine*, vol. 18, pp. 449-453, 1997.